

Supporting information

Hierarchical NiS_x/Ni₂P Nanotube Arrays with Abundant Interfaces for Efficient Electrocatalytic Oxidation of 5-Hydroxymethylfurfural

Baolong Zhang,^a Hui Fu,^b Tiancheng Mu,*^a

^a Key Laboratory of Advanced Light Conversion Materials and Biophotonics,
Department of Chemistry, Renmin University of China, Beijing 100872, China. Tel:
+86-10-62514925, E-mail: tcmu@ruc.edu.cn

^bHui Fu, College of Science, China University of Petroleum (East China), Qingdao,
266580, China. E-mail: fuhui@upc.edu.cn

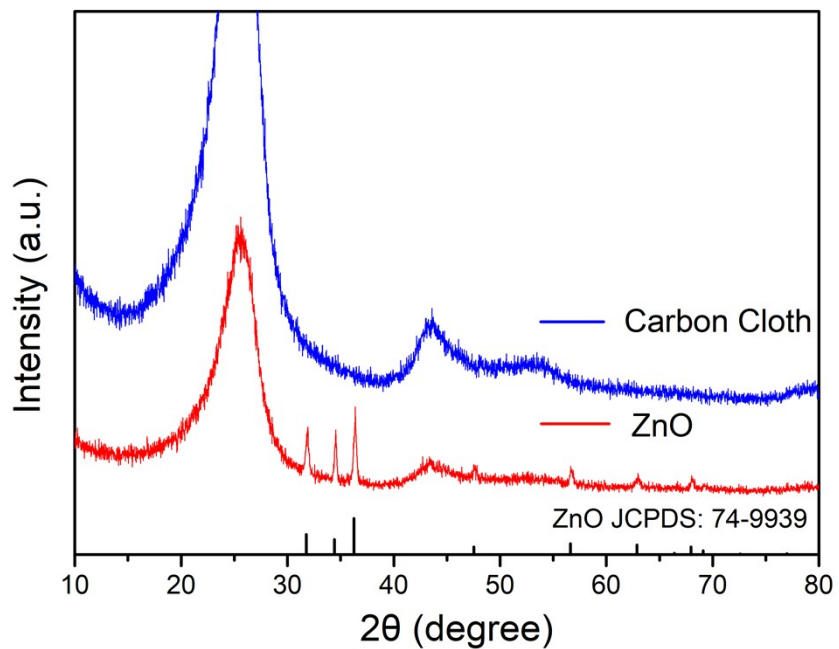


Fig. S1. The XRD pattern of ZnO and carbon cloth.

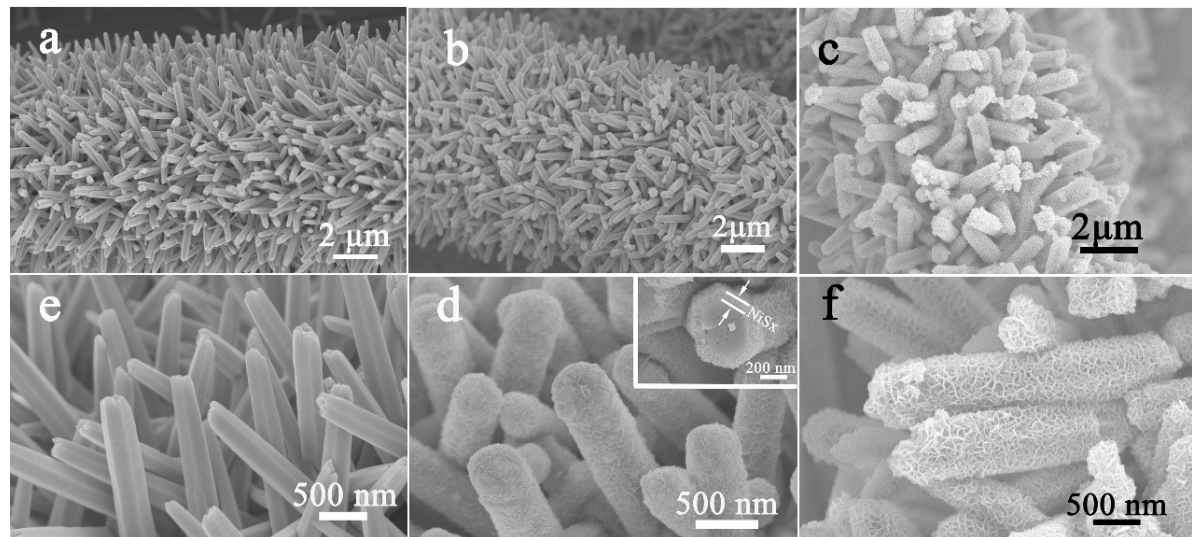


Fig. S2. SEM images of ZnO (a, e), ZnO/NiS_x (b, d), ZnO/NiS_x/Ni(OH)₂ (c, f) with different magnification.

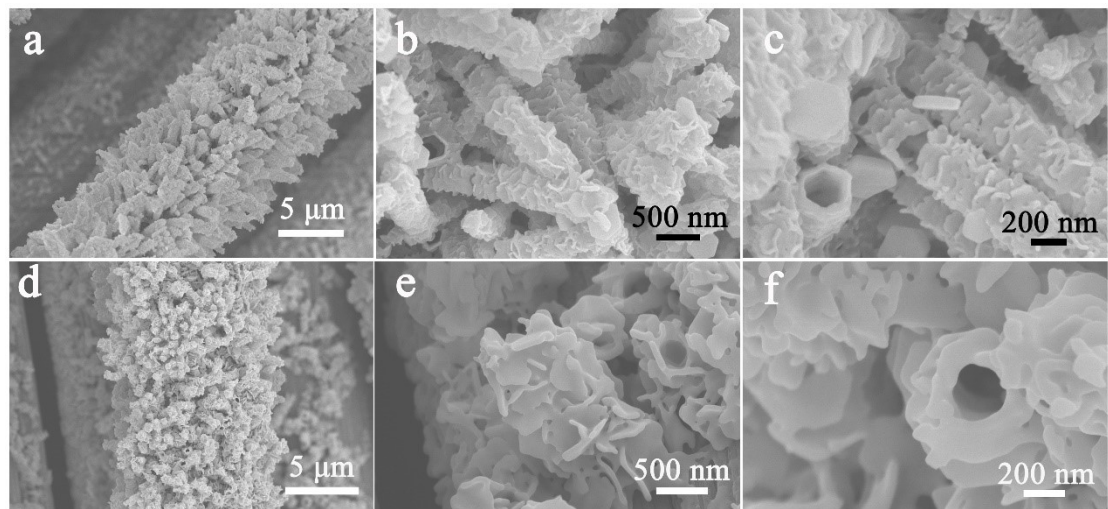


Fig. S3. SEM images of CoS_x/CoP (a, b, c) and FeS_x/FeP (d, e, f) with different magnification.

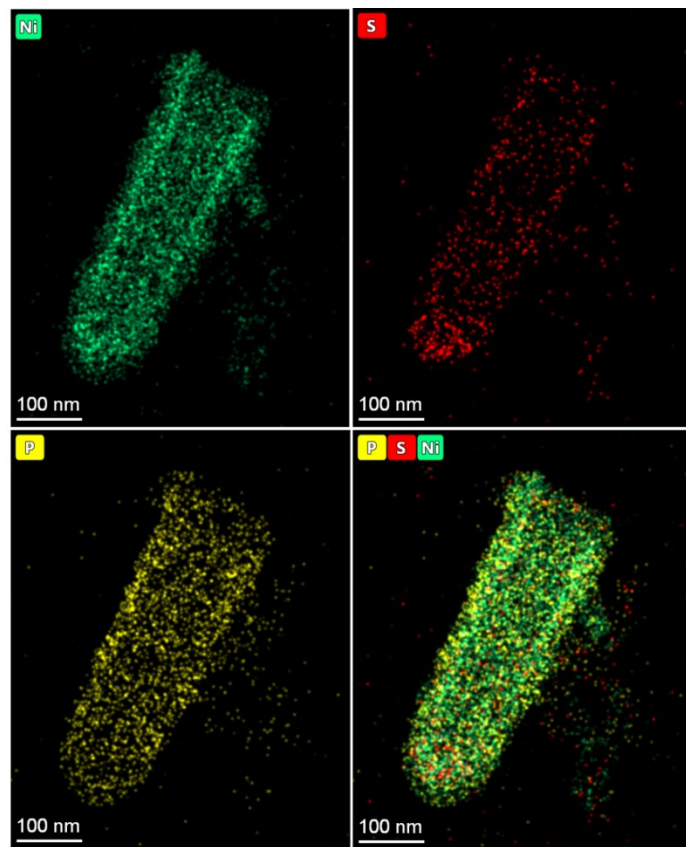


Fig. S4. STEM-EDS elemental mapping images of SNP-2.

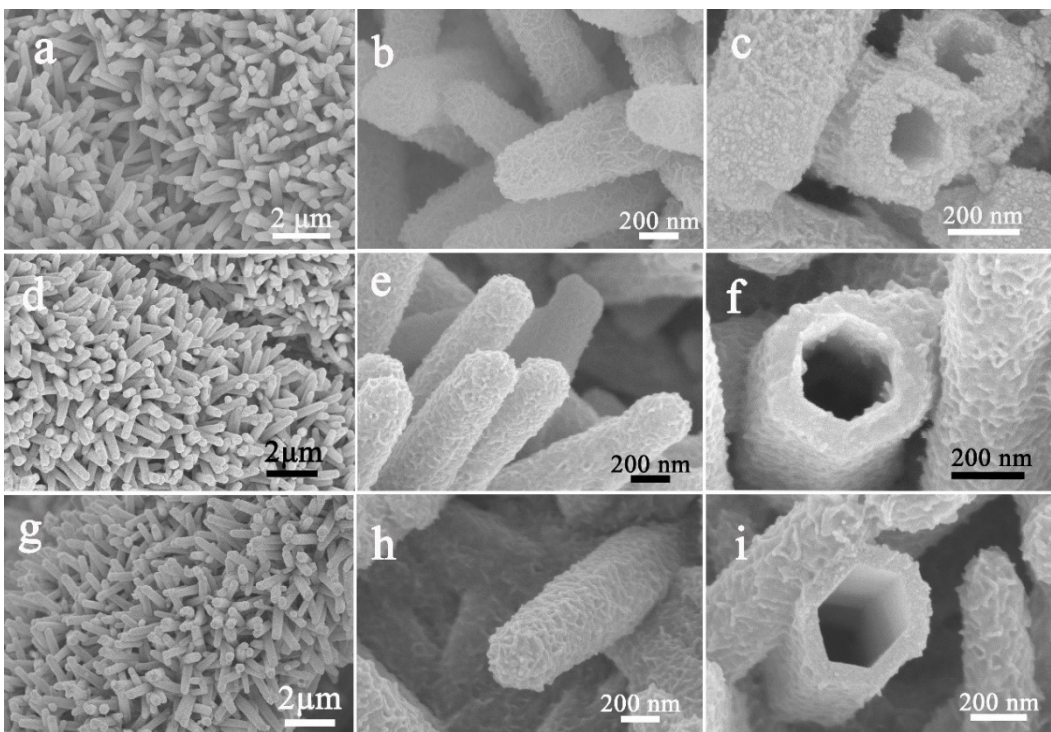


Fig. S5. SEM images of NiS_x (a, b, c), SNP-1 (d, e, f) and SNP-3 (g, h, i) with different magnification.

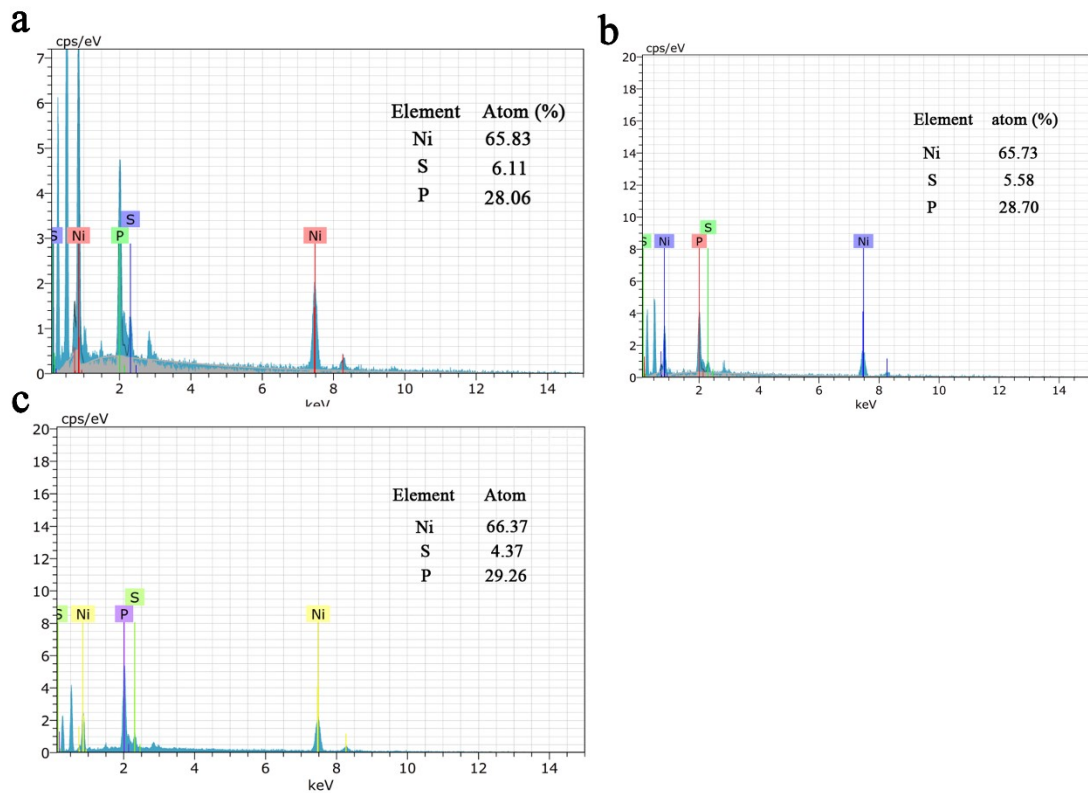


Fig. S6. EDS quantitative analysis of SNP-1, SNP-2 (b) and SNP-3 (c).

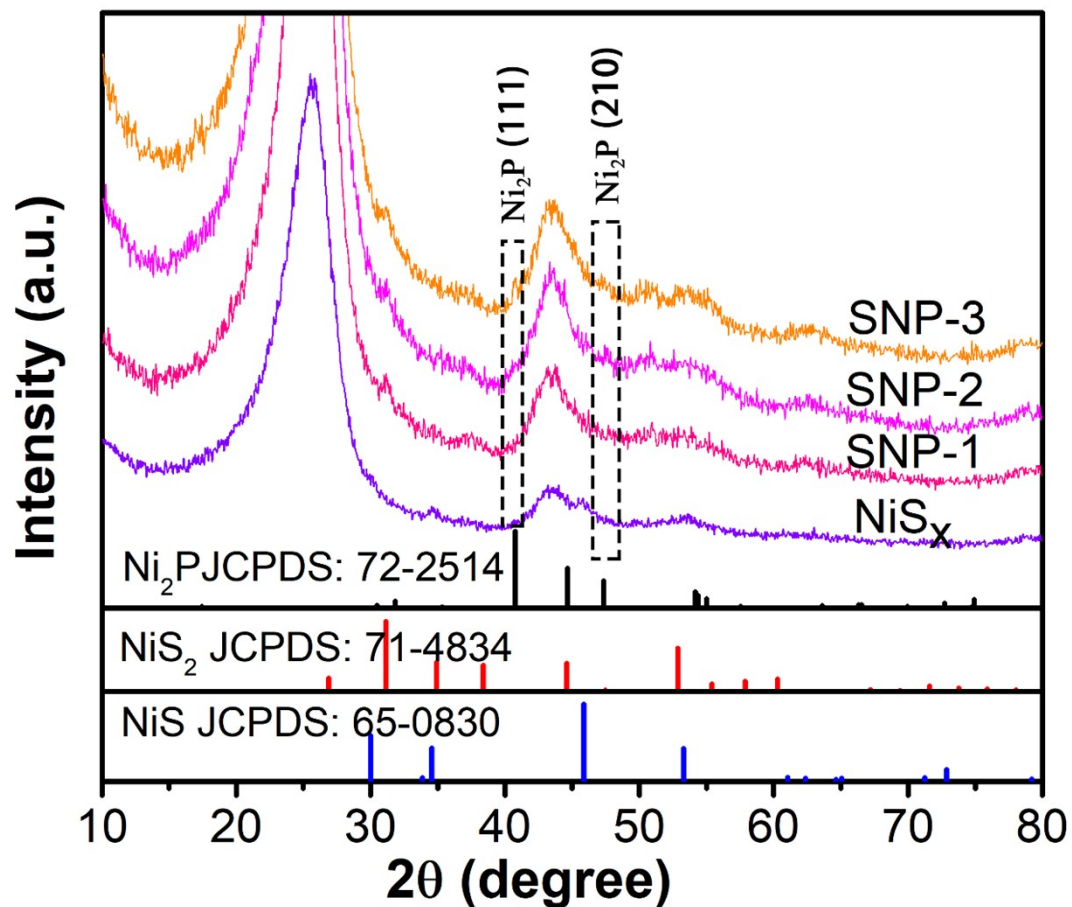


Fig. S7. The XRD patterns of NiS_x and $\text{NiS}_x/\text{Ni}_2\text{P}$ hybrid materials.

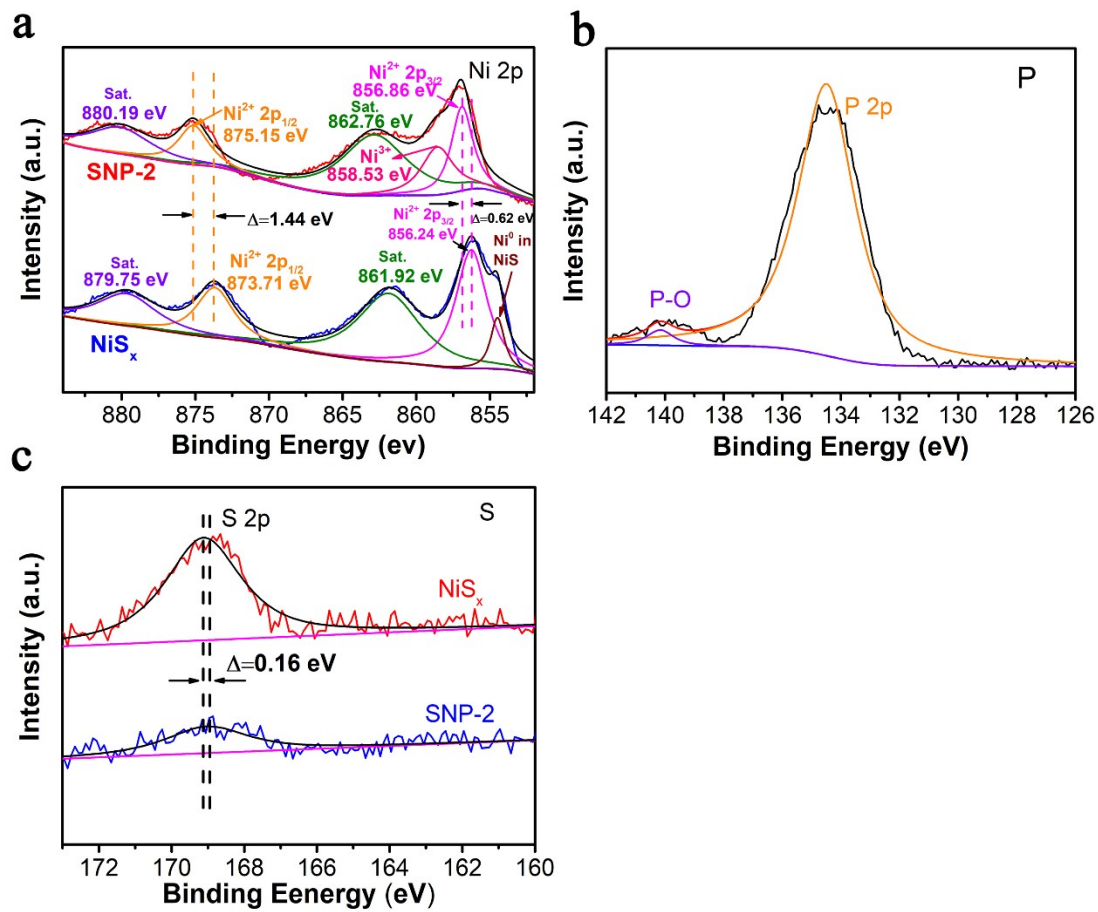


Fig. S8. XPS spectrums of SNP-2 about Ni 2p (a), P 2p (b) and S 2p (c)

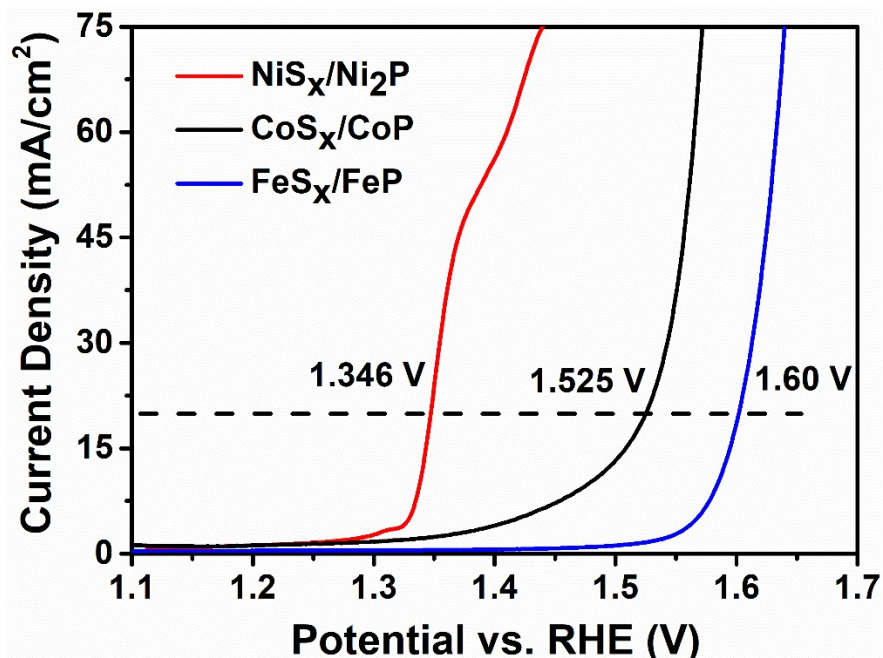


Fig. S9. LSV curves of SNP-2, CoSx/CoP and FeSx/FeP in 1 M KOH with 10 mM HMF.

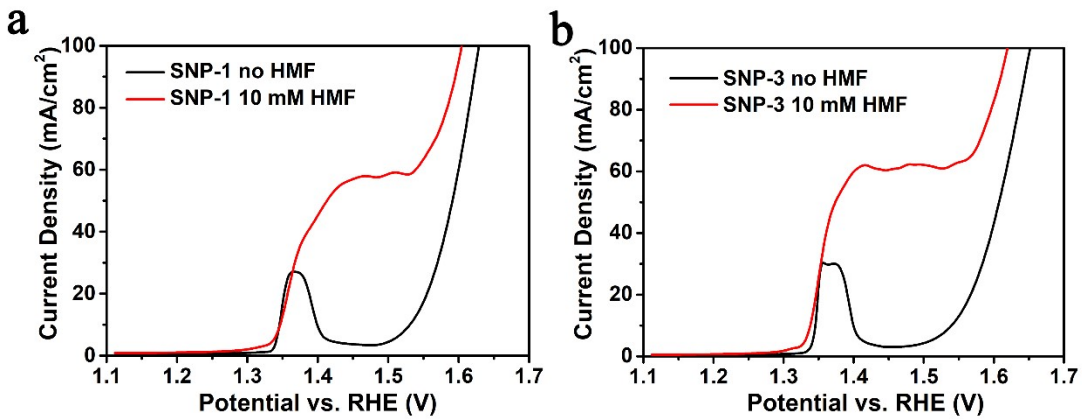


Fig. S10. LSV curves of SNP-1 (a) and SNP-3 (b) in 1 M KOH with/without HMF.

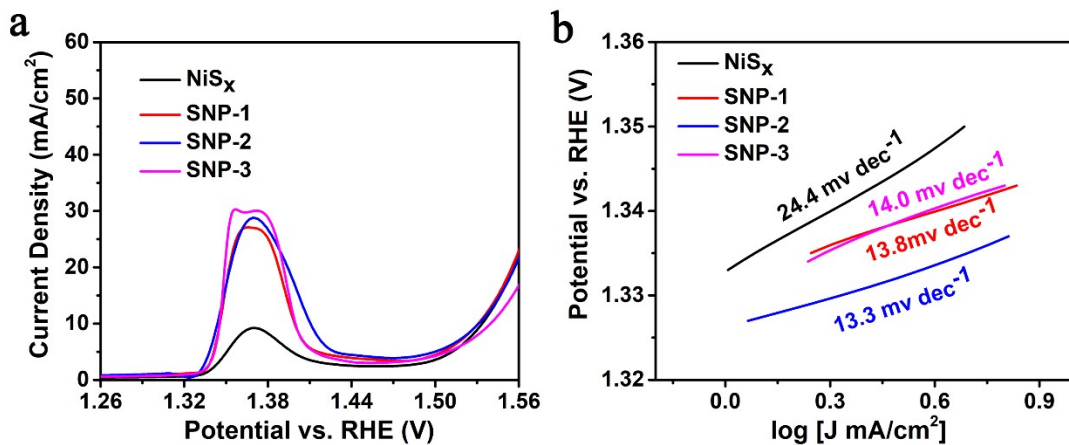


Fig. S11 LSV curves of different catalysts in 1.0 M KOH electrolyte and Tafel slopes of derived from LSVs

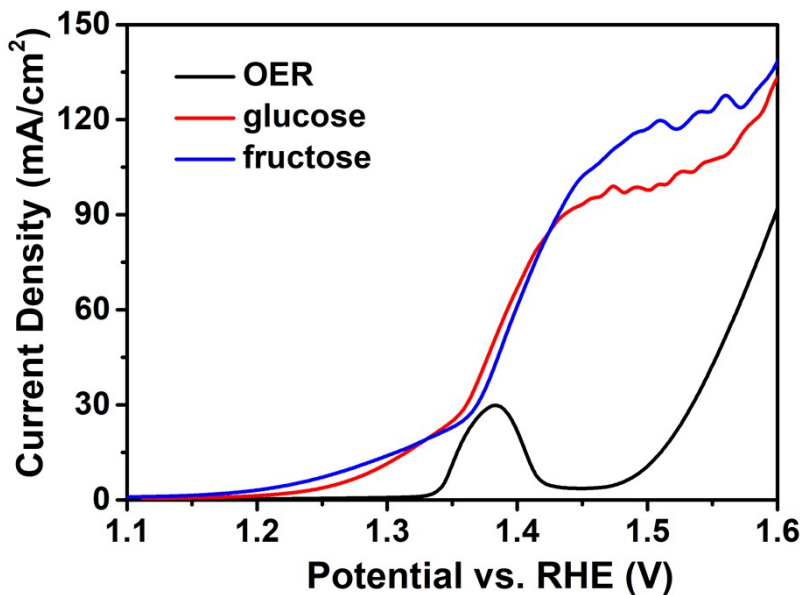


Fig. S12. LSV curves of SNP-2 in 1.0 M KOH electrolyte with 10 mM glucose (red line) and 10 mM fructose (blue line).

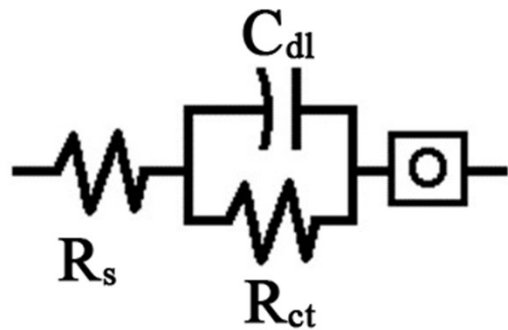


Fig. S13. Equivalent circuit applied to analyze the electrochemical impedance spectroscopy

R_s stands for the solution resistance, C_{dl} represents double layer capacitance, R_{ct} has contact with the interfacial charge transfer reaction, O stands for finite layer diffusion impedance of a planar electrode.

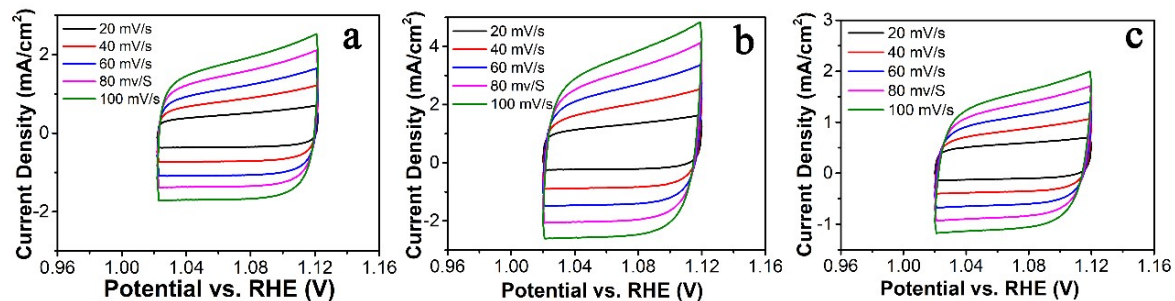


Fig. S14. The polarization curves of NiS_x (a), SNP-2 (b) in 1 M KOH with 10 mM HMF and without HMF (c) at different scan rates from 20 to 100 mV/s.

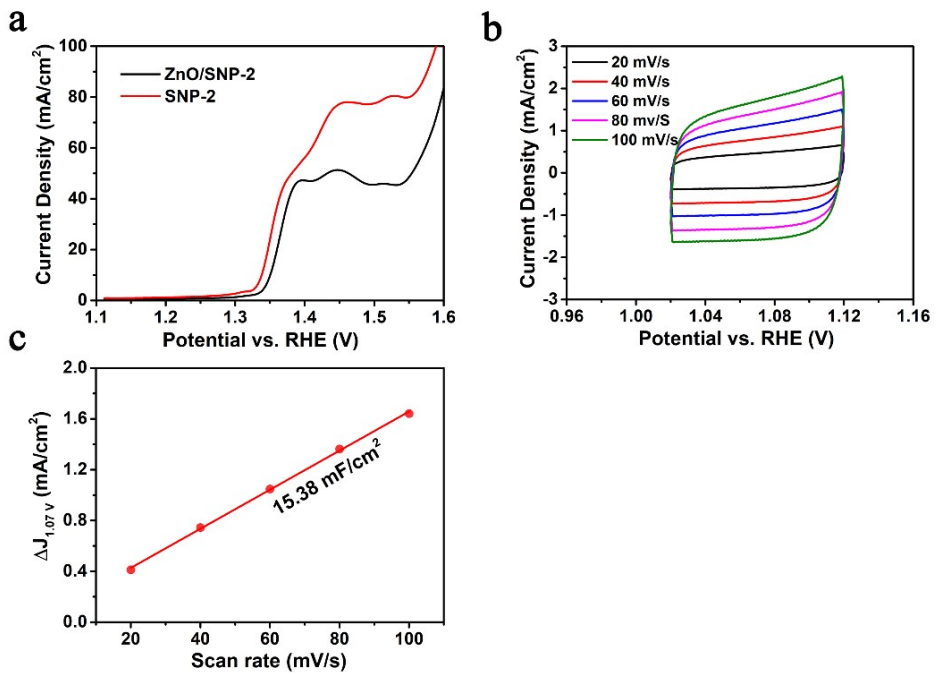


Fig. S15. (a) LSV curves of SNP-2 and ZnO/SNP-2 in 1 M KOH with 10 mM HMF. (b) The polarization curves of ZnO/SNP-2 in 1 M KOH with 10 mM HMF at different scan rates from 20 to 100 mV/s. (c) Change of current density plotted against for the scan rate at 1.07 V vs RHE for ZnO/SNP-2.

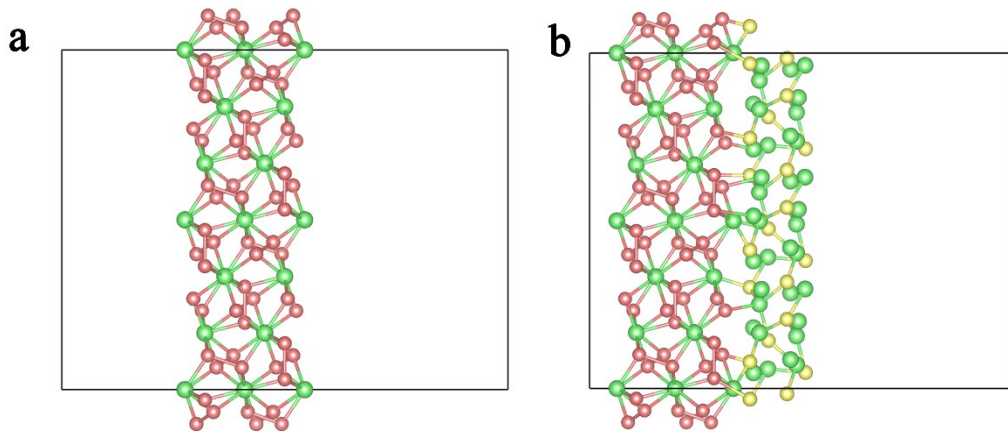


Fig. S16. a) The side view of NiS₂ (211) (Ni atom in green, S atom in red). b) The side view of the SNP-2 (Ni atom in green, S atom in red, P atom in yellow).

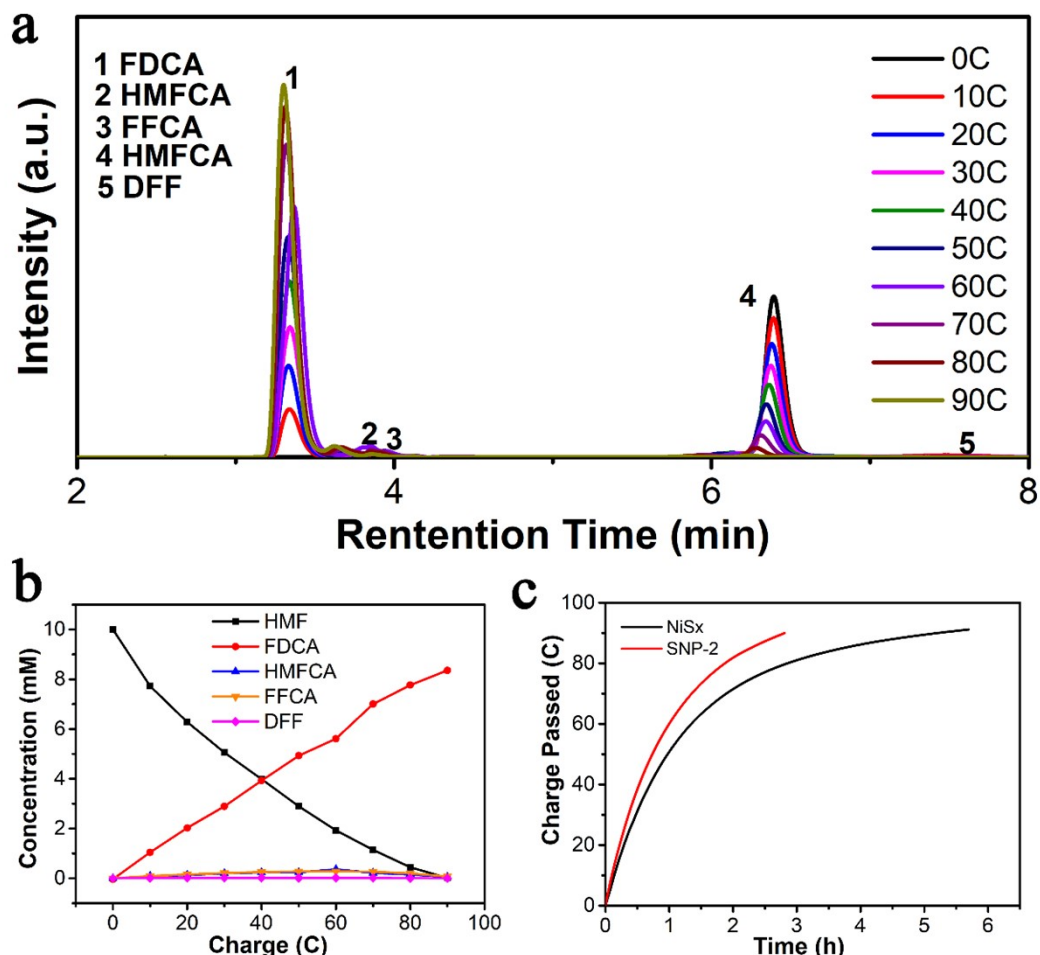


Fig. S17. HPLC traces of electrolysis of HMF oxidation catalyzed by NiS_x at 1.46 V vs RHE in 15 mL, 1 M KOH with 10 mM HMF. b) Conversion or yield of HMF and its oxidation products catalyzed by NiS_x during electrolysis. c) charge-time transients of NiS_x and SNP-2 during the electrochemical oxidation of HMF.

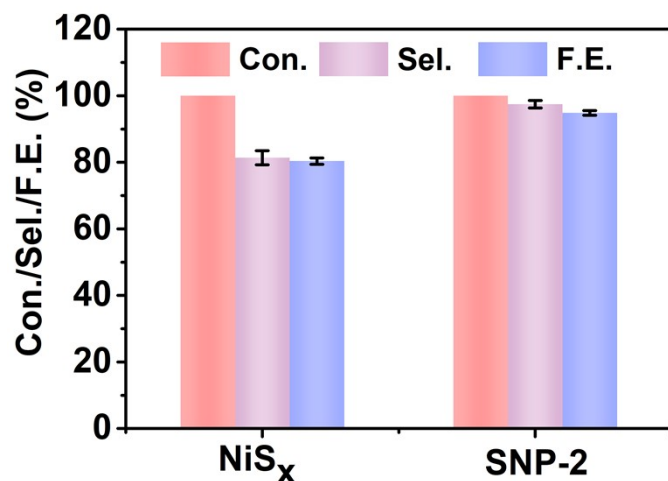


Fig. S18. Comparation of the conversion efficiency, yield and FE between SNP-2 and NiS_x.

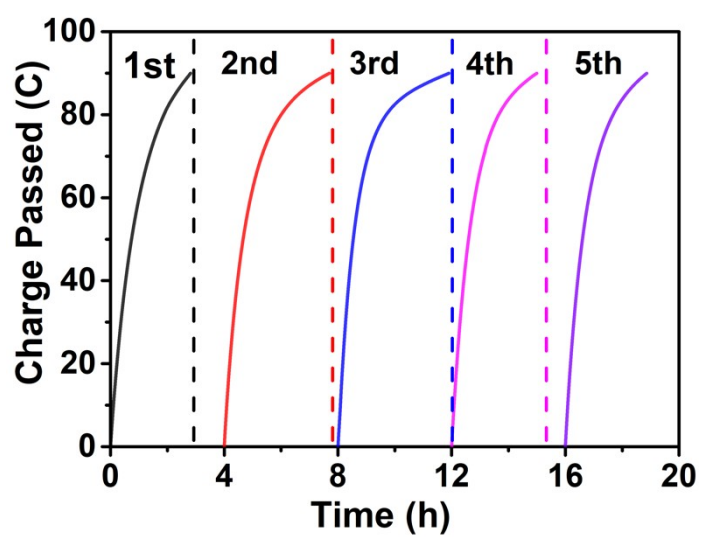


Fig. S19. charge-time transients during the electrochemical oxidation of HMF.

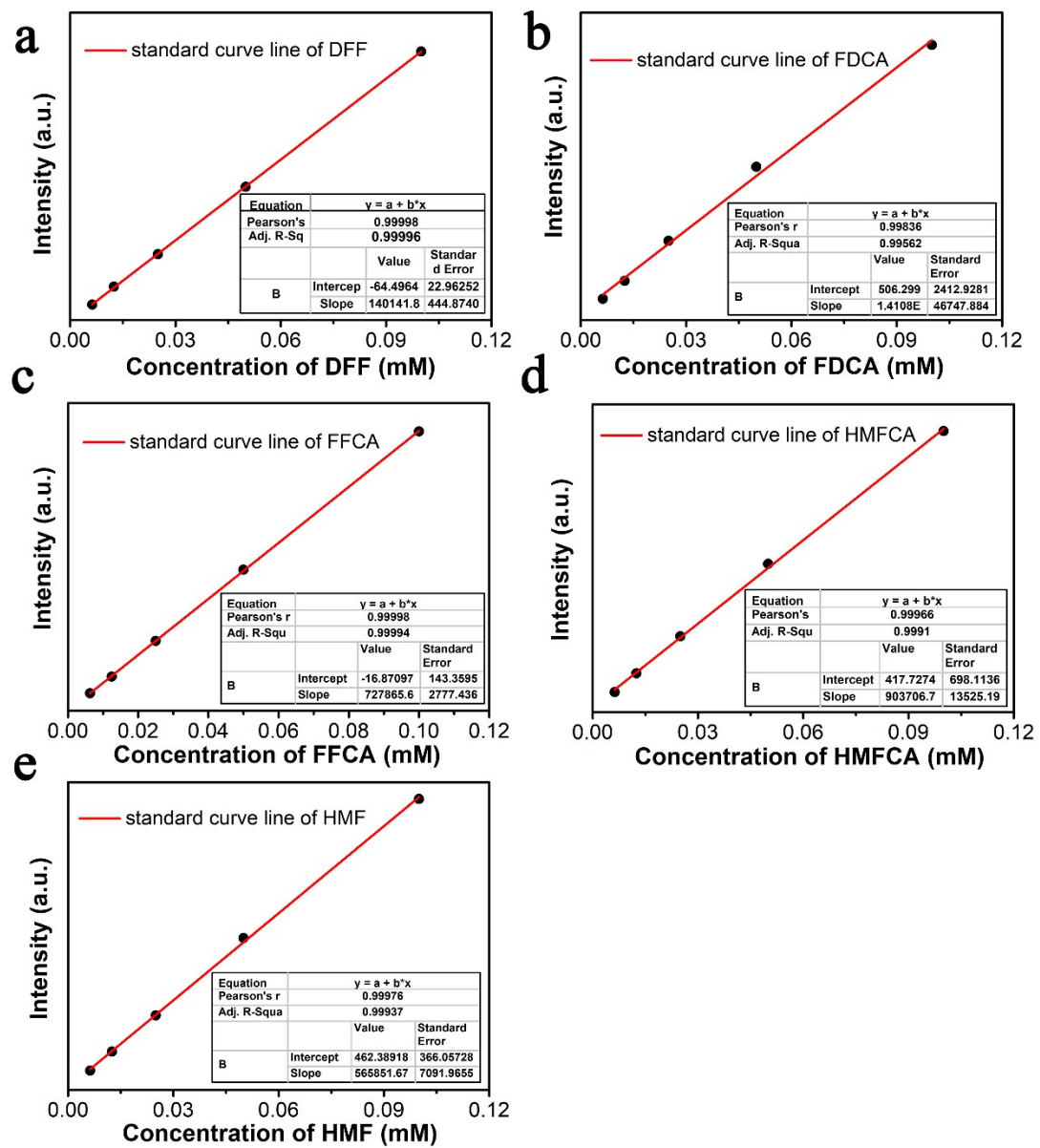


Fig. S20. Calibration of the HPLC for DFF (a), FDCA (b), FFCA (c), HMFCA (d), HMF (e).

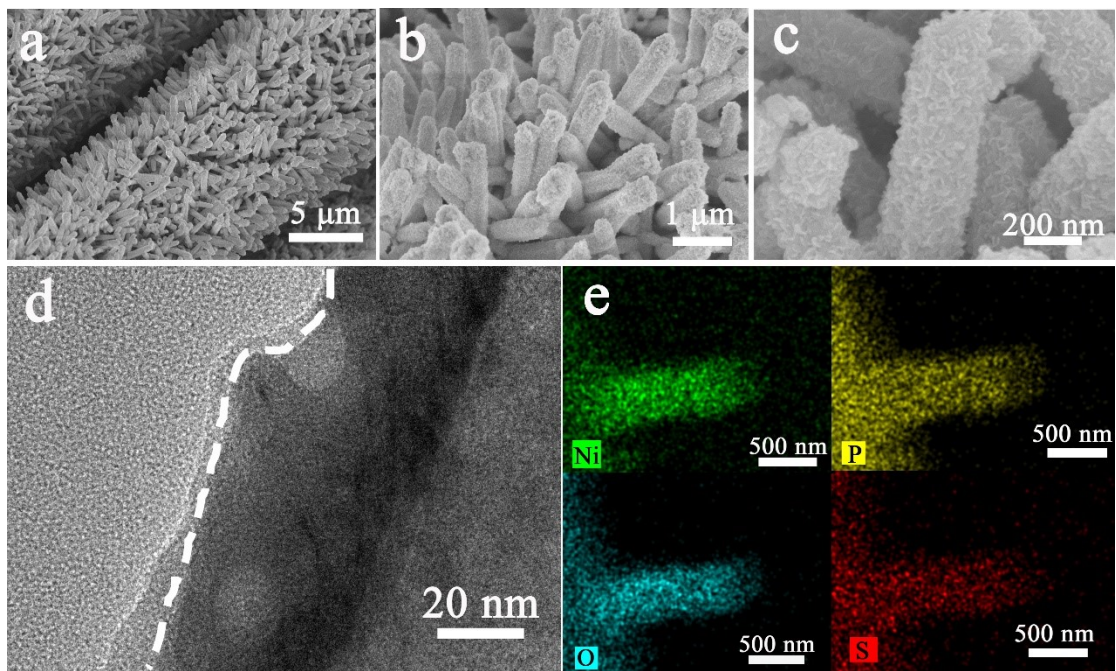


Fig. S21. SEM images of post-SNP-2 (a, b, c) with different magnification. d) TEM images of post-SNP-2. e) EDX elemental mapping of post-SNP-2.

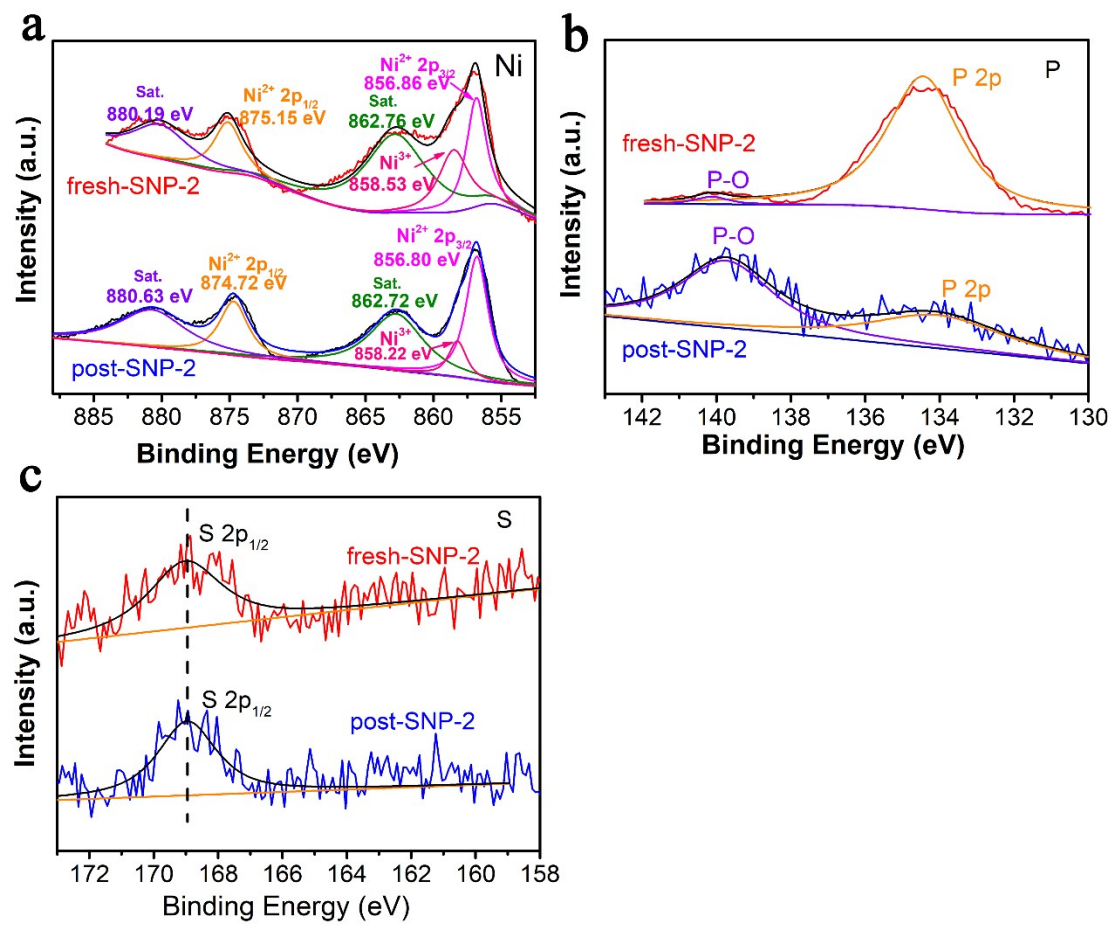


Fig. S22. XPS spectra of Ni 2p, P 2p and S 2p of pos-SNP-2 and fresh-SNP-2.

Table S1. The proposed equivalent circuit

Samples	NiS _x	SNP-2	SNP-2
Electrolyte	1.0 M KOH + 50 mM HMF	1.0 M KOH + 50 mM HMF	1.0 M KOH
R _s	1.649	1.681	1.658
C _{dl}	0.0045	0.2845	0.7335
R _{ct}	4.21	2.9	58.88
O	1.23	0.8193	7.363

Table S2. The calculated charge values (Q, q) in the case of HMF adsorbing on NiS_x and SNP-2 surfaces, respectively.

Samples	Q (Ni)	Q (S)	Q (P)	Q (HMF)
NiS _x	-14.45	14.38	0	0.065
SNP-2	-18.96	14.69	4.18	0.081

Table S3. HMF electrocatalytic performance of non-noble metal catalysts.

Catalyst	E _{onset} (V vs. RHE)	E _{j = 20 mA/cm²} (V)	FDCA	Ref.
NiS _x /Ni ₂ P	1.25	1.346	98.5	This work
Ni ₃ S ₂ /NF	~1.35	~1.36	98.0	1
Ni ₂ P NPA/NF	~1.35	~1.37	100.0	2
NiP-Al ₂ O ₃ /NF	~1.38	~1.41	99.6	3
Ni _x B	~1.38	~1.41	98.5	4
Ni ₃ N/C	1.25	1.36	98	5
NiCoBDC-NF	~1.38	~1.60	99.0	6
Ni(OH) ₂ /NF	~1.25	1.33	96.0	7
NiSe@NiO _x	~1.25	1.35	99.0	8

om-Co ₃ O ₄	1.30	~1.45	>99.8	9
NiCo ₂ O ₄	~1.23	>1.6	90.8	10
CoO-CoSe	1.30	1.38	99.0	11
CuNi(OH) ₂ /C	1.38	1.75	93.0	12
VN	1.34	1.37	96.0	13
MoO ₂ /FeP	1.35	1.38	98.6	14
NiFe LDH	1.25	1.32	98.0	15
NiCoFe LDH	1.23	1.51	84.9	16
Ni(NS)/CC	1.25	1.47	>99.0	17
t-Ni1Co1-MOF	1.25	1.28	100.0	18
Pt/Ni(OH) ₂	1.36	1.42	98.7	19

References

1. B. You, X. Liu, N. Jiang and Y. Sun, *J. Am. Chem. Soc.*, 2016, **138**, 13639-13646.
2. B. You, N. Jiang, X. Liu and Y. Sun, *Angew. Chem. Int. Ed.*, 2016, **55**, 9913-9917.
3. M. Li, L. Chen, S. Ye, G. Fan, L. Yang, X. Zhang and F. Li, *J. Mater. Chem. A*, 2019, **7**, 13695-13704.
4. S. Barwe, J. Weidner, S. Cychy, D. M. Morales, S. Dieckhöfer, D. Hiltrop, J. Masa, M. Muhler and W. Schuhmann, *Angew. Chem. Int. Ed.*, 2018, **57**, 11460-11464.
5. N. Zhang, Y. Zou, L. Tao, W. Chen, L. Zhou, Z. Liu, B. Zhou, G. Huang, H. Lin and S. Wang, *Angew. Chem. Int. Ed.*, 2019, **58**, 15895-15903.
6. M. Cai, Y. Zhang, Y. Zhao, Q. Liu, Y. Li and G. Li, *J. Mater. Chem. A*, 2020, **8**, 20386-20392.
7. J. Zhang, W. Gong, H. Yin, D. Wang, Y. Zhang, H. Zhang, G. Wang and H. Zhao, *ChemSusChem*, 2021, **14**, 2935-2942.
8. L. Gao, Z. Liu, J. Ma, L. Zhong, Z. Song, J. Xu, S. Gan, D. Han and L. Niu, *Appl. Catal. B: Environ.*, 2020, **261**, 118235.
9. C. Wang, H.-J. Bongard, M. Yu and F. Schüth, *ChemSusChem*, 2021, **14**, 1-9.
10. M. J. Kang, H. Park, J. Jegal, S. Y. Hwang, Y. S. Kang and H. G. Cha, *Appl. Catal. B: Environ.*, 2019, **242**, 85-91.
11. X. Huang, J. Song, M. Hua, Z. Xie, S. Liu, T. Wu, G. Yang and B. Han, *Green Chem.*, 2020, **22**, 843-849.
12. H. Chen, J. Wang, Y. Yao, Z. Zhang, Z. Yang, J. Li, K. Chen, X. Lu, P. Ouyang and J. Fu, *ChemElectroChem*, 2019, **6**, 5797-5801.

13. S. Li, X. Sun, Z. Yao, X. Zhong, Y. Cao, Y. Liang, Z. Wei, S. Deng, G. Zhuang, X. Li and J. Wang, *Adv. Funct. Mater.*, 2019, **29**, 1904780.
14. G. Yang, Y. Jiao, H. Yan, Y. Xie, A. Wu, X. Dong, D. Guo, C. Tian and H. Fu, *Adv. Mater.*, 2020, **32**, 2000455.
15. W.-J. Liu, L. Dang, Z. Xu, H.-Q. Yu, S. Jin and G. W. Huber, *ACS Catal.*, 2018, **8**, 5533-5541.
16. M. Zhang, Y. Liu, B. Liu, Z. Chen, H. Xu and K. Yan, *ACS Catal.*, 2020, **10**, 5179-5189.
17. X. Lu, K.-H. Wu, B. Zhang, J. Chen, F. Li, B.-J. Su, P. Yan, J.-M. Chen and W. Qi, *Angew. Chem. Int. Ed.*, 2021, **60**, 14528-14535.
18. X. Deng, M. Li, Y. Fan, L. Wang, X.-Z. Fu and J.-L. Luo, *Appl. Catal. B: Environ.*, 2020, **278**, 119339.
19. S. Wang, B. Zhou, Y. Li, Y. Zou, W. Chen, W. Zhou, M. Song, Y. Wu, Y. Lu, J. Liu and Y. Wang, *Angew. Chem. Int. Ed.*, 2021, DOI: <https://doi.org/10.1002/anie.202109211>.